Conference Proceedings

EuroSun 2016
Palma de Mallorca (Spain), 11 - 14 October 2016

Thermoeconomic Analysis of Cogeneration Systems Assisted with Solar Thermal Heat and Photovoltaics

Eduardo A. Pina[1], Miguel A. Lozano[1], Luis M. Serra[1]

[1] GITSE I3A, Universidad de Zaragoza, Maria de Luna 3, 50018, Zaragoza, Spain

Abstract

This work aims to perform a thermoeconomic analysis of a cogeneration system assisted with solar thermal heat and photovoltaic power, and determine the daily optimal operation taking into consideration the effects of thermal energy storage (TES) and hourly variations of solar radiation, energy prices and energy demands. The system is considered to be interconnected to the national electric grid, thus purchase and selling of electricity are possible. A linear programming model was developed to represent the hourly operation of the system. The results presented herein correspond to the optimal operation for a representative day in April. It was shown that the cogeneration module operates at full load throughout the day and the system sells electricity to the grid for a total of 8 hours. The marginal cost analysis showed the different situations in which heat is charged/discharged to/from the TES and how it affects the unit cost of the heat produced. It has been proposed a thermoeconomic model that incorporates a new set of equations to contribute towards a better understanding of the charge and discharge in different time periods in the TES. The obtained unit costs for internal flows and products showed that the electricity and heat produced by the cogeneration system are always cheaper than the separate conventional production (43-53% cheaper for the electricity and 19-67% cheaper for the heat).

Keywords: *cogeneration, thermal storage, solar thermal energy, photovoltaics, thermoeconomics*

1. Introduction

The increasing world energy demand as a consequence of society development, along with a growing concern about environmental issues and fossil fuel depletion have motivated the development of more efficient energy systems and that consume a greater share of renewable energy. Conventionally, the electricity consumed by buildings is purchased from the national electric grid and the heat demand is covered by onsite production, e.g. in a natural gas boiler. The building sector accounts for 40% of total energy use in the European Union. The Directive 2010/31/EU on energy performance of buildings set the framework for energy efficiency in buildings and nearly zero-energy buildings and states that new buildings must assess the technical, environmental and economic feasibility of incorporating high-efficiency alternative systems such as cogeneration (Combined Heat and Power, CHP) and of producing energy from renewable energy sources (e.g. solar thermal heat and photovoltaic power).

In CHP systems, electric (and/or mechanical) and thermal energy are produced from the same primary energy source. This combined production allows for primary energy savings and a reduction of pollutant emissions relative to the conventional separate production. By incorporating CHP systems in buildings, a shift from centralised to distributed generation takes place, which is accompanied by benefits such as reduction in transmission and distribution costs, reduction in energy dissipation, increase in energy efficiency of the system (Serra et al., 2009; Mancarella, 2014). In order to achieve the benefits described, two fundamental issues must be addressed (Lozano et al., 2010; Yokoyama et al., 2015): (i) the synthesis of the plant configuration (equipment number and capacity for each type of technology employed) and (ii) the operational planning (equipment operational strategy, energy flow rates, purchase or selling of electricity, etc.). However, the variability of energy demands in buildings as opposed to the simultaneous and often constant production in

doi:10.18086/eurosun.2016.05.03 Available at http://proceedings.ises.org

industry impose some issues to the optimal operation of the system. Moreover, the same reasoning applies to the incorporation of renewable energy sources (RES), such as photovoltaic panels and solar thermal collectors, which are characterised by low predictability and non-simultaneity between production and consumption. Therefore, it becomes convenient to incorporate thermal energy storage units, allowing a decoupling of production and consumption, reducing heat wasting to the environment and enhancing the overall performance of the system (Ashouri et al., 2013; Buoro et al., 2014).

The objective of the present work is to perform a thermoeconomic analysis of a cogeneration system assisted with solar thermal heat and photovoltaic power. A linear programming model was formulated, taking into consideration only the operational planning of the system. The daily optimal operation for a representative day in April was determined, considering the effects of thermal energy storage and hourly fluctuations of solar radiation, energy services prices and energy demands. The cost of internal flows and products of the system were assessed by analysis of marginal costs and thermoeconomic unit costs calculation.

2. System description and data elaboration

The cogeneration system analysed in the present work (Fig. 1) consists of the following productive units: (i) a cogeneration module CM, which includes a natural gas reciprocating engine and a hot water heat recovery system, producing electricity W_c and heat Q_c; (ii) an oil-fired auxiliary boiler AB, producing heat Q_a; (iii) a thermal energy storage TES that can be either charging Q_{in} or discharging Q_{out}; (iv) photovoltaic panels PV for electricity production W_{pv}; and (v) solar thermal collectors ST for heat production Q_{st}. All energy flows (in bold) are given in kW, except for the energy stored in the TES Sq, which is given in kWh.

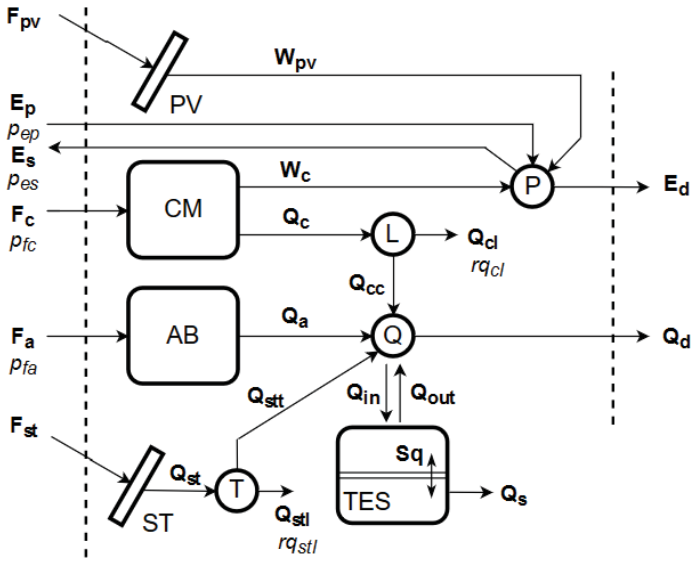

Fig. 1: Diagram of the cogeneration system

Tab. 1: Technical parameters and capacity limits of the cogeneration system's equipment

Equipment	Technical parameters	Capacity limits
Cogeneration Module (CM)	$\alpha_w = W_c/F_c = 0.35$ $\alpha_q = Q_c/F_c = 0.40$	$W_{max} = 400$ kW
Auxiliary Boiler (AB)	$\eta_q = Q_a/F_a = 0.80$	$Q_{max} = 600$ kW
Photovoltaic Panel (PV)	$P_{pv} = 0.300$ kW, $A_{pv,m} = 1.93$ m² $\eta_{pv} = 0.1538$, $\mu_T = -0.0035$ K^{-1}	$A_{pv} = 700$ m²
Solar Thermal Collector (ST)	$k_0 = 0.8170$, $k_1 = 2.2350$ W/(m²·K) $k_2 = 0.0135$ W/(m²·K²)	$A_{st} = 700$ m²
Thermal Energy Storage (TES)	$\eta_{TES} = 0.99$	$V_{max} = 1200$ kWh

Tab. 1 presents the technical parameters and capacity limits of each of the system's components. The cogeneration system was designed to attend all the electric E_d and thermal Q_d demands of a consumer centre (e.g. multifamily building). For the present work, the energy demands of a representative day in April were considered, being the total daily electric and thermal values 10,100 kWh and 19,200 kWh, respectively. As can be seen in Tab. 2, the demands and the daily operation of the system are described by 24 consecutive periods of 1-hour duration.

The system is considered to be interconnected to the national electric grid, therefore electricity can be purchased, E_p, at a price p_{ep} = 0.100 €/kWh, and sold, E_s, at a price p_{es} = 0.080 €/kWh. Natural gas and fuel oil are purchased from the market at prices p_{fc} = 0.025 €/kWh and p_{fa} = 0.020 €/kWh, respectively. There is the possibility of wasting cogenerated heat Q_{cl} and solar thermal energy Q_{stl} without cost ($rq_{cl} = rq_{stl} = 0$).

The PV and the ST are characterised by their surface areas (A_{pv} and A_{st}, respectively) and hourly specific productions (x_{pv} and x_{st}, respectively). The photovoltaic electricity W_{pv} and solar thermal Q_{st} productions can be obtained by multiplying the respective equipment area by its specific production. In order to evaluate x for each hourly period, the hourly ambient temperature T_a and the hourly radiation over tilted surface Q_r must be determined. The Erbs' correlation for ambient temperature (Erbs et al., 1983) was used to calculate the hourly T_a, using the monthly mean temperatures for the month of April from the *Guía Resumida del Clima en España 1981-2010* (AEMET, 2010). The hourly radiation Q_r over tilted surface (beam, diffuse and total) is calculated using the isotropic sky model (Duffie and Beckman, 2013). The sky clearness index can be obtained from the average daily horizontal radiation and the extraterrestrial radiation, which depends on the city latitude and the date. This index is used to calculate the daily diffuse radiation with Erbs' correlation (Erbs et al., 1982). The total horizontal radiation is hourly distributed with the Collares-Pereira and Rabl (1979) correlation, and the diffuse horizontal radiation is hourly distributed with Liu and Jordan (1960) correlation. The difference between total radiation and diffuse radiation is the direct (beam) horizontal radiation. Specific data required are: the monthly average of daily solar radiation on a horizontal surface (AENOR, 2007), latitude (41.6º for Zaragoza), surface azimuth angle (0º), reflectance of the ground (0.2) and tilt (35º for both PV and ST).

For each hourly period, x_{st} was determined by Eq. 1 using the performance coefficients from the manufacture's catalog (Tab. 1), the hourly data of the solar radiation over tilted surface Q_r, and the hourly temperature difference ΔT between the collector $T_{c,st}$ and the ambient T_a. Only the positive values of collected heat are considered. Further, $T_{c,st}$ is considered constant throughout the day and equal to 60 ºC.

$$x_{st}(h) = Max(k_0 \cdot Q_r(h) - k_1 \cdot \Delta T(h) - k_2 \cdot \Delta T(h)^2; 0) \quad \text{(Eq. 1)}$$

For each hourly period, x_{pv} was determined by Eq. 2 according to the methodology described in Duffie and Beckman (2013). The maximum power P_{pv}, the surface area $A_{pv,m}$, the module efficiency η_{pv}, and the temperature coefficient of power μ_T, were obtained from the manufacture's catalog (Tab. 1). Irradiation and cell temperature at SRC conditions are $Q_{r,SRC}$ = 1 kW/m² and $T_{c,SRC}$ = 25 ºC, respectively. Irradiation, cell temperature and ambient temperature at NOCT conditions are $Q_{r,NOCT}$ = 0.8 kW/m², $T_{c,NOCT}$ = 47 ºC and $T_{a,NOCT}$ = 20 ºC, respectively. The efficiency of power-conditioning equipment, η_e, is 0.9. The hourly cell temperature $T_{c,pv}$ and the hourly temperature correction factor F_{top} were obtained by solving Eqs. 3 and 4.

$$x_{pv}(h) = \left(P_{pv}/A_{pv,m}\right) \cdot \left(Q_r(h)/Q_{r,SRC}\right) \cdot F_{top}(h) \cdot \eta_e \quad \text{(Eq. 2)}$$

$$F_{top}(h) = 1 + \mu_T \cdot \left(T_{c,pv}(h) - T_{c,SRC}\right) \quad \text{(Eq. 3)}$$

$$T_{c,pv}(h) = T_a(h) + \left(T_{c,NOCT} - T_{a,NOCT}\right) \cdot \left(Q_r(h)/Q_{r,NOCT}\right) \cdot \left[1 - \left(\eta_{pv} \cdot F_{top}\right)/0.9\right] \quad \text{(Eq. 4)}$$

3. Optimal operation model

In order to determine the hourly operation modes that minimise the daily cost of meeting the energy demands, a linear programming model was developed and solved, as described in the following sub-sections. The LINGO modelling language and optimiser was used (LINGO, 2011).

3.1. Objective function and restrictions

The objective function is set to minimise the daily operation cost *DC* (€/day) of meeting the energy demands,

$$DC = \sum_{h=1}^{NP} HC(h) \quad \text{(Eq. 5)}$$

which is the sum of the hourly operation costs *HC(h)* of the 24 periods (*NP*) of 1-hour duration (*NHP*) that comprise the day,

$$HC(h) = \left(p_{ep}(h) \cdot E_p(h) + p_{fc}(h) \cdot F_c(h) + p_{fa}(h) \cdot F_a(h) - p_{es}(h) \cdot E_s(h)\right) \cdot NHP(h) \quad \text{(Eq. 6)}$$

subject to

Capacity limits:

CM_Wmax: $W_c(h) \leq W_{max}$ (Eq. 7)

AB_Qmax: $Q_a(h) \leq Q_{max}$ (Eq. 8)

Sqi_Vmax: $Sq_i(h) \leq V_{max}$ (Eq. 9)

Equipment efficiency:

CM_W: $\alpha_w \cdot F_c(h) - W_c(h) = 0$ (Eq. 10)

CM_Q: $\alpha_q \cdot F_c(h) - Q_c(h) = 0$ (Eq. 11)

AB_Q: $\eta_q \cdot F_a(h) - Q_a(h) = 0$ (Eq. 12)

PV_W: $A_{pv} \cdot x_{pv}(h) - W_{pv}(h) = 0$ (Eq. 13)

ST_Q: $A_{st} \cdot x_{st}(h) - Q_{st}(h) = 0$ (Eq. 14)

Balance equations:

P: $W_c(h) + W_{pv}(h) + E_p(h) - E_s(h) - E_d(h) = 0$ (Eq. 15)

L: $Q_c(h) - Q_{cc}(h) - Q_{cl}(h) = 0$ (Eq. 16)

Q: $Q_a(h) + Q_{cc}(h) + Q_{stt}(h) + Q_{out}(h) - Q_{in}(h) - Q_d(h) = 0$ (Eq. 17)

T: $Q_{st}(h) - Q_{stt}(h) - Q_{stl}(h) = 0$ (Eq. 18)

TES: $Q_{in}(h) - Q_{out}(h) - Q_s(h) + (Sq_i(h) - Sq_f(h))/NHP(h) = 0$ (Eq. 19)

The cyclical characteristic of the TES operation means that the energy stored at the beginning of an hourly period equals the energy stored at the end of the previous period (Eq. 20). Likewise, the energy stored at the beginning of the day (h = 1) must be equal to the energy stored at the end of the previous day (h = 24) (Eq. 21). The heat losses Q_s in each hourly period is a function of the TES efficiency η_{TES} and the stored energy at the beginning of the hourly period Sq_i (Eq. 22).

$$Sq_i(h) = Sq_f(h-1) \quad \text{(Eq. 20)}$$

$$Sq_i(1) = Sq_f(24) \quad \text{(Eq. 21)}$$

$$Q_s(h) = (1 - \eta_{TES}) \cdot Sq_i(h) \quad \text{(Eq. 22)}$$

3.2. Optimal operation and marginal costs

Tab. 2 presents the main flows of the system's optimal operation, for each hourly period, that brings the minimum total daily cost of 848.50 €. Positive Q_{TES} values correspond to the charged energy flow Q_{in} whereas negative values correspond to the discharged flow Q_{out}. The CM operates at full load throughout the day, while the AB modulates as needed. The daily photovoltaic production reaches 483.90 kWh, about 5% in relation to the total CM electricity production (9600 kWh). From hours 6 to 13 the system is able to sell 110.42 kWh/day of electricity to the grid, resulting in an income of 8.83 €/day; in all other hours the system purchases electricity from the grid, except for hour 5, in which the CM power production matches the electric energy demand.

Concerning the heat production, it can be seen that the solar thermal energy production peaks at hour 13, 308.42 kWh, adding up to a total daily production of 1894.70 kWh, about 17% in relation to the total cogenerated heat produced (10,971.40 kWh). Such production displaces the operation in the AB, avoiding 47.37 €/day of fuel consumption. Regarding the TES operation, for this representative day in April, it is most charged by the end of hour 4, with 416 kWh, about a third of its storage capacity. Attention should be paid to the different scenarios in which charging takes place:

Tab. 2: Optimal operation for a representative day in April

Hour	E_d[1]	Q_d[1]	T_a[2]	Q_r[3]	x_{pv}[3]	x_{st}[3]	E_p[1]	E_s[1]	W_c[1]	Q_c[1]	Q_a[1]	Sq_i[4]	Q_{TES}[1]	F_c[1]	F_a[1]	W_{pv}[1]	Q_{st}[1]
1	410	300	10.2	0	0	0	10.0	0	400	457.1	0	0	157.1	1142.9	0	0	0
2	408	300	9.6	0	0	0	8.0	0	400	457.1	0	155.6	157.1	1142.9	0	0	0
3	405	400	9.1	0	0	0	5.0	0	400	457.1	0	309.6	57.1	1142.9	0	0	0
4	402	400	8.6	0	0	0	2.0	0	400	457.1	0	363.1	57.1	1142.9	0	0	0
5	400	600	8.1	0	0	0	0	0	400	457.1	0	416.0	-142.9	1142.9	0	0	0
6	400	800	7.9	3.4	0.5	0	0	0.4	400	457.1	163.7	270.4	-179.2	1142.9	2.4	0.4	0
7	404	1000	8.1	91.3	13.4	0	0	5.4	400	457.1	600.0	90.3	57.1	1142.9	63.9	9.4	0
8	410	1200	9.0	227.1	32.8	36.4	0	13.0	400	457.1	600.0	146.0	-117.4	1142.9	159.0	23.0	25.5
9	420	1200	10.6	375.8	53.2	163.6	0	17.2	400	457.1	600.0	28.3	-28.3	1142.9	263.1	37.2	114.5
10	425	1200	12.6	516.1	71.5	285.3	0	25.1	400	457.1	543.1	0	0	1142.9	361.3	50.1	199.7
11	435	1000	14.5	625.7	85.2	381.7	0	24.6	400	457.1	275.7	0	0	1142.9	438.0	59.6	267.2
12	445	1000	16.2	685.7	92.2	436.3	0	19.5	400	457.1	237.4	0	0	1142.9	480.0	64.5	305.4
13	459	700	17.4	685.7	91.8	440.6	0	5.3	400	457.1	0	0	65.6	1142.9	480.0	64.3	308.4
14	461	600	18.3	625.7	84.0	394.5	2.2	0	400	457.1	0	64.9	133.3	1142.9	438.0	58.8	276.2
15	455	700	18.8	516.1	69.9	306.8	6.1	0	400	457.1	0	196.2	-28.1	1142.9	361.3	48.9	214.8
16	439	800	18.9	375.8	51.6	192.3	2.9	0	400	457.1	41.8	166.4	-166.4	1142.9	263.1	36.1	134.6
17	425	1000	18.4	227.1	31.7	69.2	2.8	0	400	457.1	525.6	0	31.2	1142.9	159.0	22.2	48.4
18	418	1000	17.3	91.3	13.0	0	8.9	0	400	457.1	600.0	30.9	57.1	1142.9	63.9	9.1	0
19	413	1000	15.9	3.4	0.5	0	12.7	0	400	457.1	600.0	87.2	57.1	1142.9	2.4	0.4	0
20	412	1200	14.5	0	0	0	12.0	0	400	457.1	600.0	142.9	-142.9	1142.9	0	0	0
21	413	900	13.3	0	0	0	13.0	0	400	457.1	442.9	0	0	1142.9	0	0	0
22	414	700	12.3	0	0	0	14.0	0	400	457.1	242.9	0	0	1142.9	0	0	0
23	416	600	11.6	0	0	0	16.0	0	400	457.1	142.9	0	0	1142.9	0	0	0
24	411	600	10.9	0	0	0	11.0	0	400	457.1	142.9	0	0	1142.9	0	0	0
Day[4]	10,100	19,200	-	5050.2	691.3	2706.7	126.5	110.4	9600	10,971.4	6358.8	-	24.9	27,428.6	3535.14	483.9	1894.7

given in: [1] kW, [2] ºC, [3] W/m^2, [4] kWh.

- Excess heat production: in hours 1 to 4, 13 and 14 the heat production from solar thermal collector and cogeneration module surpasses the thermal energy demand. The surplus heat stored for later consumption allows a reduction in the conventional heat production;
- Conventional heat required: in hours 7 and 17 to 19 the system must store energy in order to guarantee supply in hours of peak thermal demand (1200 kWh), e.g. hours 8, 9 and 20. Therefore, the AB is put into operation at the closest feasible period to the discharge, as to reduce heat losses to a minimum.

Dual prices obtained from the linear programming model help to unravel the marginal costs of internal flows and products, and to evaluate the economic impact of changes in demand or operational condition of the equipment (Lozano et al., 2009b).

Regarding the optimal operation, from hours 6 to 13, when the system is selling electricity to the grid, supplying an additional unit of electricity to the consumer centre means reducing selling by the same amount, therefore its marginal cost equals the selling price ($\lambda E_d = p_{es} = 0.080$ €/kWh); on the other hand, when the system matches the electric demand (hour 5) or purchases electricity from the grid (the rest of the time), the marginal cost of the electricity corresponds to the purchasing price ($\lambda E_d = p_{ep} = 0.100$ €/kWh).

Supplying an additional unit of heat to the consumer centre will always result in an increase in the production of the AB because solar thermal energy is a non-dispatchable resource and the CM already operates at full load throughout the day. Therefore, the important thing to notice is when this production takes place. Fig. 2 presents the 24 hourly periods and their respective marginal costs in €/kWh. The grey circles represent periods in which the AB is modulating. In such periods, the additional unit of heat is produced and consumed at the same hourly period, thus its marginal cost is the cost of producing 1 kW in the AB ($\lambda Q_d = p_{fa}/\eta_{AB} = 0.025$ €/kWh). The red circles indicate periods in which the dispatchable equipment (CM and AB) are not able to increase their productions (CM and AB operate at full load) and thus the deficit of heat must be produced in an earlier period and stored. In these cases, the AB will have to produce more than 1 kW as to compensate for the storage heat losses, resulting in a marginal cost that equals the cost of producing 1 kW plus heat losses in the AB. The blue circles correspond to periods of excess heat. Consuming an additional unit of heat in such periods means that one less unit is stored in the TES, so, in a later period, the AB will have to increase its production in not 1 kW, but less. Thus, the marginal cost will be the cost of producing 1 kW minus heat losses in the AB. The marginal costs of interconnected periods (red and blue circles) can be calculated by Eq. 23, which relates the cost of producing 1 kW in the AB, the TES efficiency and the storage time between the period k of AB production and the period h of additional unit of heat consumption.

$$\lambda Q_d(h) = \left(p_{fa}/\eta_{AB}\right) \cdot \eta_{TES}^{(k-h)} \qquad \text{(Eq. 23)}$$

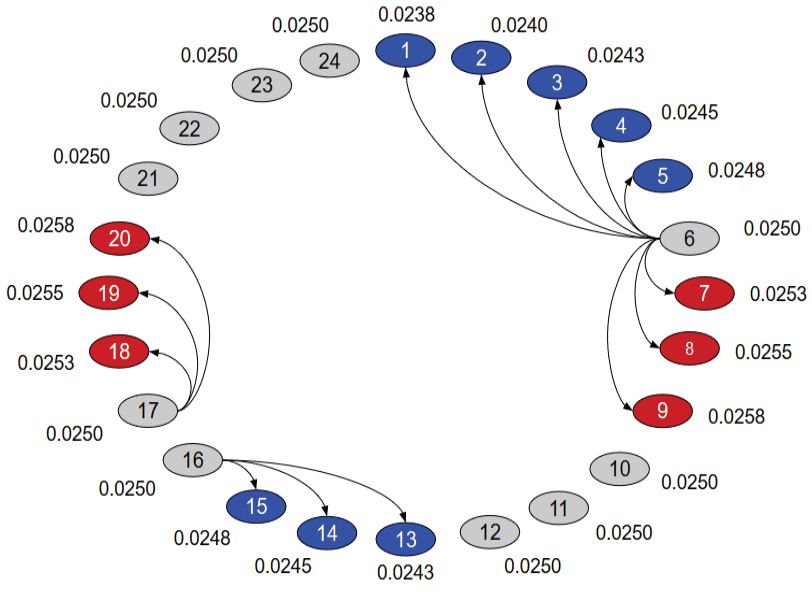

Fig. 2: Hourly marginal costs of the heat supplied to the consumer centre in €/kWh

4. Interconnection Between Hourly Periods

As stated by Chicco and Mancarella (2009), the effective combination of the different alternatives of production can bring forward enhanced benefits in terms of economic profitability, among others. In the analysed system, the thermal energy demand can be met by heat production in the CM, AB and/or ST at different productions costs. Because of the TES, heat can be produced and consumed at the same hourly period or produced and stored for later consumption. Therefore, as important as evaluating how much energy must be charged and discharged from the TES at each period, is knowing its source period. Only then the cost of the discharged flow can be traced back up to its production.

The optimal operation model described in section 3.1 gives the amount of heat that must be charged or discharged into the TES in each hourly period. In order to broaden this view and allow for a better understanding of how charge and discharge periods are interconnected through the TES, it was proposed to include a new set of equations in the model. It should be noted that such considerations do not change the results obtained; only more detailed information about the optimal processes of heat charge and discharge is revealed.

The diagram presented in Fig. 3 can be taken as example to clarify the interconnection between charging and discharging periods: the heat discharged in period z, $Q_{out}(z)$, is composed of virtual energy flows originated in three different earlier periods: OUT(i,z), OUT(j,z) and OUT(k,z) (Eq. 24); the pair (i,z) meaning i as the source period and z the destination period. Therefore, the heat stored in period i, $Q_{in}(i)$, may be divided into several virtual flows IN(i,x) that are going to be discharged in later periods, OUT(i,x) (Eq. 25). On account of heat losses, the discharge flow is always lower than the charge one (Eq. 26). The heat losses LOSS are assessed at the end of each period for each pair, and are proportional to the stored volume and duration (Eq. 27); the notation (i,z,j) means i as the source period, z as the destination period, and j the period in which the heat losses are being assessed. Thus, the longer the storage duration, the greater the heat losses along the pair, as can be seen by comparing pairs (i,z) and (k,z), the former with three LOSS flows and the latter with only one. The total heat losses of each period Q_s can be calculated as the sum of all LOSS flows in that period (Eq. 28), thus replacing Eq. 22.

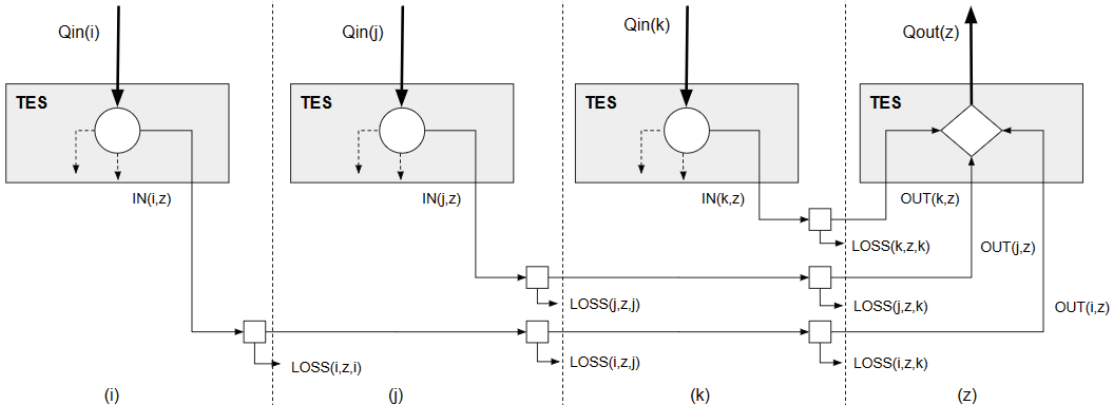

Fig. 3: Diagram for the charging and discharging of the TES

$$Q_{out}(h) = \sum_{i \neq h} OUT(i,h) \quad \text{(Eq. 24)}$$

$$Q_{in}(h) = \sum_{z \neq h} IN(h,z) \quad \text{(Eq. 25)}$$

$$IN(i,z) = OUT(i,z) + \sum_{h=i}^{z-1} LOSS(i,z,h) \quad \text{(Eq. 26)}$$

$$\sum_{h=i}^{j} LOSS(i,z,h) = IN(i,z) \cdot \left(1 - \eta_{TES}{}^{(j-i+1)}\right) \text{ for all } j = i, \ldots\ldots, z-1 \quad \text{(Eq. 27)}$$

$$Q_s(h) = \sum_{i,z} LOSS(i,z,h) \quad \text{(Eq. 28)}$$

The chart in Fig. 4 presents, for each relevant pair of periods (j,k), the charged energy IN, the discharged energy OUT and the heat losses LOSS between them. Because heat losses increase with storage time, as explained earlier, the model seeks to keep energy stored for the minimum time necessary in order to guarantee supply, meaning that the first unit of energy to be charged must be the first unit of energy to be discharged. Even though the model may infringe this rule once in a while, e.g. pairs (1,9) and (2,6), the optimal operation still stands, as both pairs form a loop in a way that shortening a pair and extending the other, e.g. (1,6) and (2,9), would provide equivalent heat losses.

Pair (j,k)		1	2	3	4	5	6	7	8	9	10...12	13	14	15	16	17	18	19	20	21...24
(1,5)	IN, OUT	148,72				142,86														
	LOSS	1,49	1,47	1,46	1,44															
(1,9)	IN, OUT	8,43								7,77										
	LOSS	0,08	0,08	0,08	0,08	0,08	0,08	0,08	0,08											
(2,6)	IN, OUT		128,22				123,16													
	LOSS		1,28	1,27	1,26	1,24														
(2,8)	IN, OUT		6,87						6,46											
	LOSS		0,07	0,07	0,07	0,07	0,07	0,07												
(2,9)	IN, OUT		22,06							20,56										
	LOSS		0,22	0,22	0,22	0,21	0,21	0,21	0,21											
(3,8)	IN, OUT			57,14					54,34											
	LOSS			0,57	0,57	0,56	0,55	0,55												
(4,6)	IN, OUT				57,14		56,01													
	LOSS				0,57	0,57														
(7,8)	IN, OUT							57,14	56,57											
	LOSS							0,57												
(13,16)	IN, OUT											65,56			63,62					
	LOSS											0,66	0,65	0,64						
(14,15)	IN, OUT												28,38	28,10						
	LOSS												0,28							
(14,16)	IN, OUT												104,91		102,82					
	LOSS												1,05	1,04						
(17,20)	IN, OUT															31,21			30,28	
	LOSS															0,31	0,31	0,31		
(18,20)	IN, OUT																57,14		56,01	
	LOSS																0,57	0,57		
(19,20)	IN, OUT																	57,14	56,57	
	LOSS																	0,57		
Qin(z)		157,1	157,1	57,1	57,1	0,0	0,0	57,1	0,0	0,0	0,0	65,6	133,3	0,0	0,0	31,2	57,1	57,1	0,0	0,0
Qout(z)		0,0	0,0	0,0	0,0	142,9	179,2	0,0	117,4	28,3	0,0	0,0	0,0	28,1	166,4	0,0	0,0	0,0	142,9	0,0
Qs(z)		1,6	3,1	3,7	4,2	2,7	0,9	1,5	0,3	0,0	0,0	0,7	2,0	1,7	0,0	0,3	0,9	1,4	0,0	0,0

Fig. 4: Heat flows between relevant pairs of periods through the TES

5. Thermoeconomic Analysis and Cost Allocation

In energy systems, resources are consumed in order to produce certain qualities to the internal flows until the desired final products are obtained. Thermoeconomics allows the cost formation process to be transparent throughout the system, from energy resources to final products (Lozano and Valero, 1993).

In the cogeneration system analysed herein (Fig. 1) the possibility of selling electricity to the grid provides an income ($p_{es} \cdot E_s$) that reduces the operation cost. As the CM and the PV are the two productive units that can produce electricity, it was proposed to proportionally distribute E_s between both equipment according to their power productions. By doing so, the benefit of selling electricity to the grid could be incorporated to the internal flow costs of cogenerated W_{cc} and photovoltaic W_{pvv} electricity produced by the system. For each hourly period, the parameter γ, defined by Eq. 29, was used to determine the cogenerated E_{cs} and photovoltaic E_{pvs} electricity sold to the grid.

$$\gamma(h) = W_{pv}(h)/\left(W_{pv}(h) + W_c(h)\right) \quad \text{(Eq. 29)}$$

$$E_{pvs}(h) = \gamma(h) \cdot E_s(h) \quad \text{(Eq. 30)}$$

$$E_{cs}(h) = (1 - \gamma(h)) \cdot E_s(h) \quad \text{(Eq. 31)}$$

In order to properly carry out a thermoeconomic analysis, it is essential to identify the correct productive structure of the system (Lozano et al., 2011). Fig. 5 presents the productive structure devised for the thermoeconomic analysis, showing the energy flows in bold, the market prices of the resources in italic and the unit costs of internal flows and final products.

For each hourly period, all energy flows of the system and the prices of the commercial energy sources consumed are known (p_{ep} = 0.100 €/kWh, p_{es} = 0.080 €/kWh, p_{fc} = 0.025 €/kWh, p_{fa} = 0.020 €/kWh). There is no cost related to the dissipation of heat to the ambient (rq_{cl} = 0 and rq_{stl} = 0) and to the heat losses in the TES

(c_{Qs} = 0). The solar resource is obtained at zero cost (c_{Fst} = 0 and c_{Fpv} = 0). Thus, there remain 9 unit costs to be determined (c_{Wpvv}, c_{Wcc}, c_{Qcc}, c_{Qa}, c_{Qstt}, c_{Qin}, c_{Qout}, c_{Ed}, c_{Qd}).

Applying the cost conservation principle as described in Lozano et al. (2009a) to PV+V, ST+T, AB and P brings c_{Wpvv}, c_{Qstt}, c_{Qa} and c_{Ed}, respectively. There remain 5 unit costs to be determined (c_{Wcc}, c_{Qcc}, c_{Qin}, c_{Qout}, c_{Qd}). To complete the calculation of unit costs the following auxiliary equations are proposed.

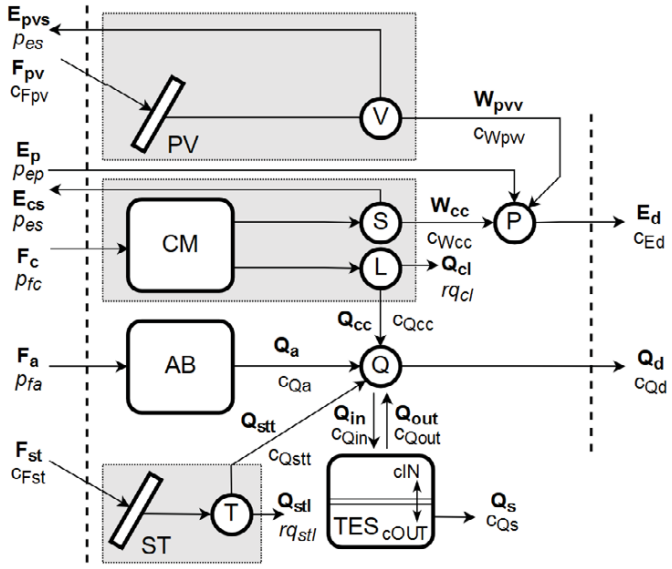

Fig. 5: Productive structure of the cogeneration system for the thermoeconomic analysis

Apart from the cost balance in CM+S+L, another equation is needed in order to determine the unit costs of the cogenerated products (c_{Wcc} and c_{Qcc}). The cogeneration subsystem is characterised by concurrent production of energy services, which is achieved through the energy integration of the process occurring in the equipment. Such a high level of integration hinders the determination of a unique distribution of the resource consumed F_c towards the obtained products W_{cc} and Q_{cc}. Considering an equal share of benefits, it was proposed (Lozano et al., 2011) to apply the same discount d to both products of the cogeneration subsystem (see Fig. 5) with respect to the cost of their conventional separate production: the purchasing price of electricity, $(c_w)_{ref}$ = p_{ep} = 0.100 €/kWh, for W_{cc}, and the cost of producing heat in the AB, $(c_q)_{ref}$ = p_{fa}/η_{AB} = 0.025 €/kWh, for Q_{cc}.

$$d(h) = 1 - c_{Wcc}(h)/(c_W)_{ref} = 1 - c_{Qcc}(h)/(c_Q)_{ref} \quad \text{(Eq. 32)}$$

$$c_{Wcc}(h)/p_{ep} = c_{Qcc}(h)/(p_{fa}/\eta_{AB}) \quad \text{(Eq. 33)}$$

The cost balance in junction Q will change according to the operation of the TES. When the TES is charging, an accepted rule can be applied, which establishes that the unit cost of several flows obtained from a homogeneous flow is the same (Lozano and Valero, 1993). This same rule can be applied to distribute c_{Qin} between the virtual IN flows (see section 4). Hence, Eq. 34 follows:

$$c_{Qin}(h) = c_{Qd}(h), \text{ when } Q_{in}(h) > 0 \quad \text{(Eq. 34)}$$

When the TES is discharging, the cost balance in Q gives c_{Qd}. In this case, the unit cost of the discharged flow c_{Qout} must be known. It can be determined by applying the cost conservation principle to Eq. 24.

$$c_{Qout}(h) = (\sum_{i \neq h} c_{OUT}(i,h) \cdot OUT(i,h))/Q_{out}(h), \text{ when } Q_{out}(h) > 0 \quad \text{(Eq. 35)}$$

The unit cost of the discharged energy c_{OUT} in a pair (h,j) (see section 4) can be determined by considering the increase in the unit cost of the charged energy c_{IN} in the same pair due to heat losses:

$$c_{IN}(h,j) = c_{Qin}(h) \quad \text{(Eq. 36)}$$

$$c_{OUT}(h,j) = c_{IN}(h,j) \cdot IN(h,j)/OUT(h,j), \text{ when } OUT(h,j) > 0 \quad \text{(Eq. 37)}$$

Tab. 3 presents the unit costs obtained for internal flows and products of the system. It was verified that the

unit costs of the final products c_{Ed} and c_{Qd} are always lower than the cost of their separate production.

Tab. 3: Unit costs of the main internal flows and products of the system, in €/kWh

Hour	cEd	cWcc	cWpvv	cQd	cQa	cQcc	cQin	cQout	d[1]
1	0.0566	0.0556	-	0.0139	-	0.0139	0.0139	-	0.4444
2	0.0564	0.0556	-	0.0139	-	0.0139	0.0139	-	0.4444
3	0.0561	0.0556	-	0.0139	-	0.0139	0.0139	-	0.4444
4	0.0558	0.0556	-	0.0139	-	0.0139	0.0139	-	0.4444
5	0.0556	0.0556	-	0.0140	-	0.0139		0.0145	0.4444
6	0.0555	0.0555	-0.0001	0.0163	0.0250	0.0139		0.0144	0.4446
7	0.0540	0.0553	-0.0011	0.0202	0.0250	0.0138	0.0202	-	0.4470
8	0.0518	0.0550	-0.0025	0.0194	0.0250	0.0137		0.0174	0.4504
9	0.0498	0.0548	-0.0033	0.0181	0.0250	0.0137		0.0149	0.4522
10	0.0479	0.0545	-0.0047	0.0165	0.0250	0.0136	-	-	0.4555
11	0.0468	0.0545	-0.0045	0.0131	0.0250	0.0136	-	-	0.4551
12	0.0466	0.0547	-0.0035	0.0122	0.0250	0.0137	-	-	0.4527
13	0.0476	0.0553	-0.0009	0.0083	-	0.0138	0.0083	-	0.4466
14	0.0487	0.0556	-	0.0087	-	0.0139	0.0087	-	0.4444
15	0.0502	0.0556	-	0.0094	-	0.0139		0.0087	0.4444
16	0.0513	0.0556	-	0.0111	0.0250	0.0139		0.0087	0.4444
17	0.0530	0.0556	-	0.0189	0.0250	0.0139	0.0189	-	0.4444
18	0.0553	0.0556	-	0.0202	0.0250	0.0139	0.0202	-	0.4444
19	0.0569	0.0556	-	0.0202	0.0250	0.0139	0.0202	-	0.4444
20	0.0569	0.0556	-	0.0202	0.0250	0.0139		0.0203	0.4444
21	0.0570	0.0556	-	0.0194	0.0250	0.0139	-	-	0.4444
22	0.0571	0.0556	-	0.0177	0.0250	0.0139	-	-	0.4444
23	0.0573	0.0556	-	0.0165	0.0250	0.0139	-	-	0.4444
24	0.0568	0.0556	-	0.0165	0.0250	0.0139	-	-	0.4444
Day	0.0532	0.0554	-0.0020	0.0162	0.0250	0.0138	0.0141	0.0145	0.4464

[1] Discount applied to the cogenerated products, nondimensional.

Photovoltaic production and/or selling of electricity contribute to reducing c_{Ed}. In fact, at hour 12, when the system is selling electricity to the grid and the PV production is highest, c_{Ed} reaches its lowest value, 53% cheaper than p_{ep}. On the other hand, c_{Ed} peaks at hour 23, when there is no PV production and the system is purchasing electricity from the grid. Then, c_{Ed} is only 43% cheaper than p_{ep}. Considering the unit cost of the heat supplied to the consumer centre, it plunges at hour 13, when solar thermal production is highest, attaining a 67% reduction relative to the cost of producing heat in the AB. The highest c_{Qd} takes place at hour 20, when there is no solar thermal production, the AB works at full load and the TES is in discharging mode. At this hour, the reduction in c_{Qd} is of about 19%.

Regarding the products of the cogeneration subsystem, c_{Wcc} and c_{Qcc}, their unit costs are aprox. 45% cheaper than the cost of their conventional separate productions. This is due to the discount d applied, as explained earlier. The discount values increase between hours 6 and 13 because of the selling of cogenerated electricity to the grid. The income associated with the selling of E_{cs} is incorporated into the cogenerated products, reducing their unit costs and increasing the discount in those hours, as can be seen from Tab. 3.

By considering free of charge the solar resource, the income due to the selling of photovoltaic electricity to the grid results in negative unit costs of the photovoltaic electricity supplied to the system c_{Wpvv}, which contributes to lowering even further c_{Ed}.

Similar to Fig. 4, Fig. 6 presents the internal costs of the charged and discharged heat from the TES, for each pair (j,k) and for each hourly period z.

Pair (j,k)	1	2	3	4	5	6	7	8	9	10...12	13	14	15	16	17	18	19	20	21...24
(1,5) cIN, cOUT	0,0139				0,0145														
(1,9) cIN, cOUT	0,0139								0,0151										
(2,6) cIN, cOUT		0,0139				0,0145													
(2,8) cIN, cOUT		0,0139						0,0148											
(2,9) cIN, cOUT		0,0139							0,0149										
(3,8) cIN, cOUT			0,0139					0,0146											
(4,6) cIN, cOUT				0,0139		0,0142													
(7,8) cIN, cOUT							0,0202	0,0204											
(13,16) cIN, cOUT											0,0083			0,0085					
(14,15) cIN, cOUT												0,0087	0,0087						
(14,16) cIN, cOUT												0,0087		0,0088					
(17,20) cIN, cOUT															0,0189			0,0195	
(18,20) cIN, cOUT																0,0202		0,0206	
(19,20) cIN, cOUT																	0,0202	0,0204	
cQin(z)	0,0139	0,0139	0,0139	0,0139	0,0000	0,0000	0,0202	0,0000	0,0000	0,0000	0,0083	0,0087	0,0000	0,0000	0,0189	0,0202	0,0202	0,0000	0,0000
cQout(z)	0,0000	0,0000	0,0000	0,0000	0,0145	0,0144	0,0000	0,0174	0,0149	0,0000	0,0000	0,0000	0,0087	0,0087	0,0000	0,0000	0,0000	0,0203	0,0000

Fig. 6: Internal costs of charged and discharged heat from the TES

As can be seen from Fig. 6, the unit cost of the heat discharged from the TES c_{Qout} is always lower than the cost of its separate production (p_{fa}/η_{AB} = 0.025 €/kWh). Looking into each section (j,k), it can be noted the considerable variation of c_{Qout} throughout the day, which reaches a 133% difference between its highest and lowest values. Such variations are due to the nature of the charged heat. Different system equipment produce heat at different unit costs, e.g. c_{Qa} = 0.025 €/kWh, c_{Qcc} = 0.0139 €/kWh and c_{Qstt} = 0 €/kWh. Because the CM operates at full load at all hourly periods, the unit cost of the charged heat will be closer or farther from c_{Qcc} depending on its share in the total heat produced. For example, for hours 1 to 4, $c_{Qin} = c_{Qcc}$ because all the thermal energy produced by the system comes from the CM. In hours 7 and 17 to 19, there is a higher share of conventional than cogenerated heat (e.g. 57% Q_a and 43% Q_{cc}, for hour 7), resulting in a c_{Qin} closer to c_{Qa}. On the other hand, in hours 13 and 14 the free solar resource allows the c_{Qin} to be lower than c_{Qcc} (e.g. 62% Q_{cc} and 38% Q_{stt}, for hour 14).

6. Closure

Cogenerated Heat and Power systems have been progressively used in commercial and residential buildings in order to reduce primary energy consumption and costs of the energy services relative to the separate conventional production. The present work proposed to analyse a cogeneration system assisted with solar thermal heat and photovoltaics, located in Zaragoza (Spain). The daily optimal operation for a representative day in April was obtained by a linear programming model developed in LINGO.

The marginal cost analysis evinced the fundamental difference between (i) storing excess heat for later consumption because it is a better option than wasting it into the environment, and (ii) producing heat to be stored in order to guarantee supply in a later period.

Thermoeconomic analysis was used to determine the cost of internal flows and final products of the system. It has been shown that the electricity and heat produced by the cogeneration system were always cheaper than the separate conventional production, e.g. electricity purchase from the national electric grid and onsite heat production in an auxiliary boiler. However, it must be noted that the way in which costs are allocated to products will influence the consumer's behaviour. The incorporation of a TES adds a new dimension to the cost allocation problem: not only it requires to know from which equipment the heat produced comes from, but also in which time period it was produced.

7. Acknowledgments

This work was developed in the frame of the research project ENE2014-57262-R, partially funded by the Spanish Government (Energy Program), the Government of Aragon (Spain) and the European Union (FEDER Program). The authors also want to acknowledge the program "Ciência sem Fronteiras" offered by CNPq (Brazil).

8. References

AEMET, 2010. Guía Resumida del Clima en España 1981-2010 [WWW Document]. URL http://www.aemet.es/en/conocermas/recursos_en_linea/publicaciones_y_estudios/publicaciones/detalles/guia_resumida_2010 (accessed 8.30.16).

AENOR, 2007. Norma UNE 94003: Datos climáticos para el dimensionado de instalaciones solares térmicas.

Ashouri, A., Fux, S.S., Benz, M.J., Guzzella, L., 2013. Optimal design and operation of buildings services using mixed-integer linear programming techniques. Energy, Vol. 59, pp. 365-376.

Buoro, D., Pinamonti, P., Reini, M., 2014. Optimization of a distributed cogeneration system with solar district heating. Applied Energy, Vol 124, pp. 298-308.

Chicco, G., Mancarella, P., 2009. Distributed multi-generation: A comprehensive view. Renew. Sustain. Energy Rev. 13, 535–551.

Collares-Pereira, M., Rabl, A., 1979. The average distribution of solar radiation: correlations between diffuse and hemispherical and between daily and hourly insolation values. Solar Energy, Vol. 22, pp. 155–184.

Directive 2010/31/EU of the European Parliament and the Council of 19 May 2010 on the energy performance of buildings. Official Journal of the European Union 18.06.2010.

Duffie, J.A., Beckman, W.A., 2013. Solar Engineering of thermal processes, 4th Ed. Wiley.

Erbs, D.G., Klein, S.A., Duffie, J.A., 1982. Estimation of diffuse radiation fraction for hourly, daily and monthly-average global radiation. Solar Energy, Vol. 28, pp. 293–302.

Erbs, D.G., Klein S.A., Beckman, W.A., 1983. Estimation of degree-days and ambient temperature bin data from monthly-average temperatures. ASHRAE J. 25, 60–65.

LINGO, 2011. The modeling language and optimizer. Lingo Systems [WWW Document]. URL http://www.lindo.com/ (accessed 8.11.16).

Liu, B.Y.H., Jordan, R.C., 1960. The interrelationship and characteristic distribution of direct diffuse and total solar radiation. Solar Energy Vol. 4, pp. 1–19.

Lozano, M.A., Valero, A., 1993. Theory of the exergetic cost. Energy, Vol. 18, pp. 939-960.

Lozano, M.A., Carvalho, M., Ramos, J.C., Serra, L.M., 2009a. Thermoeconomic analysis of simple trigeneration systems. Int. J. Thermodyn. 12, 147–153.

Lozano, M.A., Carvalho, M., Serra, L.M., 2009b. Operational strategy and marginal costs in simple trigeneration systems. Energy 34, 2001–2008.

Lozano, M.A., Ramos, J.C., Serra, L.M., 2010. Cost optimization of the design of CHCP (combined heat, cooling and power) systems under legal constraints. Energy, Vol. 35, pp. 794-805

Lozano, M.A., Carvalho, M., Serra, L.M., 2011. Allocation of economic costs in trigeneration systems at variable load conditions. Energy and Buildings, Vol. 43, pp. 2869-2881.

Mancarella, P., 2014. MES (multi-energy systems): An overview of concepts and evaluation models. Energy 65, 1–17.

Serra, L.M., Lozano, M.A., Ramos, J.C., Ensinas, A.V., Nebra, S.A., 2009. Polygeneration and efficient use of natural resources. Energy, Vol. 34, pp. 575-586.

Yokoyama, R., Shinano, Y., Taniguchi, S., Ohkura, M., Wakui, T., 2015. Optimization of energy supply systems by MILP branch and bound method in consideration of hierarchical relationship between design and operation. Energy Conversion and Management, Vol. 92, pp. 92-104.